

Pre-onset land surface processes and ‘internal’ interannual variabilities of the Indian summer monsoon

Subodh K. Saha · Subhadeep Halder ·
K. Krishna Kumar · B. N. Goswami

Received: 16 October 2009 / Accepted: 20 July 2010 / Published online: 13 August 2010
© Springer-Verlag 2010

Abstract It is proposed that, land–atmosphere interaction around the time of monsoon onset could modulate the first episode of climatological intraseasonal oscillation (CISO) and may generate significant ‘internal’ interannual variation in the Indian summer monsoon rainfall. The regional climate model RegCM3 is used over Indian monsoon domain for 27 years of control simulation. In order to prove the hypothesis, another two sets of experiment are performed using two different boundary conditions (El Niño year and non-ENSO year). In each of these experiments, a single year of boundary conditions are used repeatedly year after year to generate ‘internal’ interannual monsoon variability. Simulation of monsoon climate in the control model run is found to be in reasonably good agreement with observation. However, large rainfall bias is seen over Arabian Sea and Bay of Bengal. The interannual monsoon rainfall variability are of the same order in two experiments, which suggest that the external influences may not be important on the generation of ‘internal’ monsoon rainfall variability. It is shown that, a dry (wet) pre-onset land-surface condition increases (decreases) rainfall in June which in turn leads to an anomalous increase (decrease) in seasonal (JJAS) rainfall. The phase and amplitude of CISO are modulated during May–June and beyond that the modulation of CISO is quite negligible. Though the pre-onset rainfall is unpredictable, significant modulation of the post-onset monsoon rainfall by it can be exploited to improve predictive skill within the monsoon season.

1 Introduction

The interannual variability (IAV) of Indian summer monsoon plays a dominant role on the economy, agriculture and day-to-day life of people in the region. Unlike in most part of the tropics, the predictability of seasonal rainfall in the Indian summer monsoon region is limited by the ‘internal’ IAV or climate noise (Sperber and Palmer 1996; Sugi and Kawamura 1997; Goswami 1998; Ajayamohan and Goswami 2003; Goswami and Xavier 2005; Kumar et al. 2005; Krishnan et al. 2009). Understanding the physical processes responsible for the ‘internal’ IAV is the key towards developing improved forecast methodology. Vigorous intraseasonal oscillations (ISOs) that manifest in active and break spells of the Indian monsoon and arise from convective feedback (Goswami and Shukla 1984) may be responsible for generating the ‘internal’ IAV (Goswami and Ajayamohan 2001; Goswami and Xavier 2005). There is, however, considerable gap in our understanding of how the ISOs generate the internal IAV. While seasonal bias of the ISO anomalies contributes to the seasonal mean, it explains only one half of the amplitude of internal IAV (Goswami and Xavier 2005). Here, we propose another mechanism through which ISOs could generate internal IAV of the monsoon and demonstrate it from an internal IAV simulation with a regional climate model (RCM).

Some of the monsoon ISOs are locked with the annual cycle and form the climatological intraseasonal oscillation (CISO) (Lau et al. 1988; Wang and Xu 1997; Kang et al. 1999). CISO of monsoon rainfall represents a predictable component of the monsoon ISO and accounts for up to 20–40% of ISO amplitude (Sahas and Goswami 2008). Changes in the amplitude and phase of the CISO could also contribute to the seasonal mean and lead to a component of

S. K. Saha (✉) · S. Halder · K. K. Kumar · B. N. Goswami
Indian Institute of Tropical Meteorology, Pune 411008, India
e-mail: subodh@tropmet.res.in; subodhsaha@yahoo.com

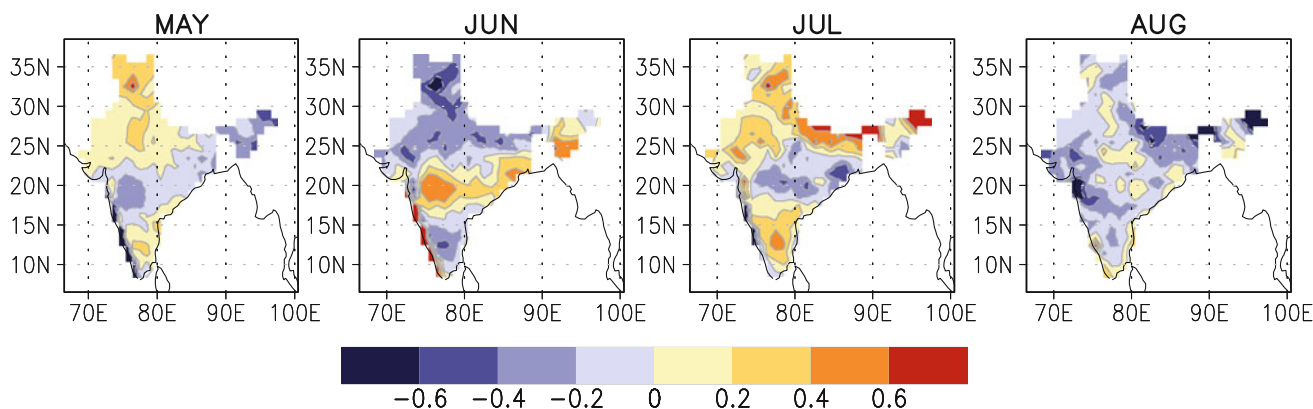


Fig. 1 Monthly composite of ‘internal’ rainfall anomaly (mm day^{-1}) based on IMD daily gridded data (1951–2007). ‘Internal’ rainfall is calculated by removing first four harmonics (including mean) from daily data and then averaging over the months

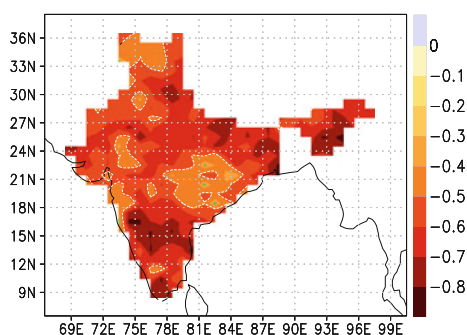


Fig. 2 Correlation between May and June ‘internal’ rainfall based on IMD daily gridded data (1951–2007). Correlation is significant at 99% level except for a few points marked in *green color*. *White dashed contour* represent correlation value of -0.5

‘internal’ IAV of the monsoon. The northward propagation of CISO can be seen clearly in the monthly composite of ‘internal’ rainfall during the month May–July (Fig. 1). Here the ISOs whose phase and amplitude vary randomly from year to year are nullified by each other in the monthly composite. But the ISOs which are phase locked with annual cycle remain and hence represents the CISO. The negative phase of CISO arrives over central India (CI) during the month of May and it becomes positive during June over the same region.

We propose that internal variability through land–atmosphere interaction can modulate the first episode of monsoon CISO around the transition period from pre-onset to post-onset and could generate significant ‘internal’ IAV. For example, pre-onset convective rain can reduce the land–ocean temperature gradient and hence the strength of the low-level wind. Therefore, a delayed onset and/or reduction in June rainfall may be expected. Similarly, a drier pre-onset (May) is likely to lead to an early onset and/or stronger low level moisture convergence and higher rain

in June. If this is true, a negative correlation between ‘internal’ component of May and June rainfall anomalies may be expected. This is indeed true as shown in Fig. 2. In most of the area the correlation is significant at 99% level. It shows indeed an increase in June rainfall due to decrease in May rainfall and the vice versa. We hypothesize that land–atmosphere feedback through pre-onset rainfall variability can modulate the phase and amplitude of CISO and the strong negative correlation between May and June rainfall anomaly is primarily due to the modulation of CISO. Thus a part of ‘internal’ interannual monsoon rainfall variability may arise due to pre-onset rainfall variability.

To test the hypothesis, a RCM forced by observed and reanalysis data is used. The ideas behind selection of a RCM for this study are the following: (a) it can isolate the influences generated out of the monsoon region. Otherwise, the external influences, generated in the remote region by the local feedback processes may interact with the internal monsoon dynamics and may produce more variability. Probably it was one of the reasons behind the large monsoon rainfall variability (of the order of natural variability) generated in internal simulation experiment by AGCM (e.g. Goswami 1998; Krishnan et al. 2009). (b) High resolution simulation can be performed using limited computational resources, where the regional-scale feedback processes are also included.

Control simulations of about 27 years are carried out to validate the model monsoonal climatology. Boundary data of 1982 and 1989 are used in two separate simulations, each for 31 years. Detailed descriptions of model and experiment design are given in Sect. 2. Methodology and observed data used for this study are described in Sect. 3. In Sect. 4, results from control simulation and comparison with observations are given. Results from fixed boundary condition are described in Sect. 5 and the conclusions are stated in Sect. 6.

2 Model and experimental design

The RCM RegCM3 (Pal et al. 2007) is used in this study. The dynamical core of RegCM is equivalent to the hydrostatic version of the fifth-generation Pennsylvania State University National Center for Atmospheric Research (NCAR), US, Meso-scale Model (MM5). The physical parameterizations employed in the simulations include the radiative transfer package of the NCAR Community Climate Model version 3 (CCM3, Kiehl et al. 1996), the non-local boundary layer scheme by Holtslag et al. (1999) and mass flux cumulus cloud scheme of Grell (1993) with Fritsch and Chappell (1980) closure. Land-surface processes are described using biosphere–atmosphere transfer scheme (BATS) (Dickinson et al. 1993). For this study, the standard model configuration with 18 vertical levels in the atmosphere (sigma coordinate) and 60 km horizontal resolution with Normal Mercator map projection is used. The model domain covers the Indian subcontinent and its surrounding land and ocean part (40.2°–116.3°E, 10.8°S–47.7°N).

In the lateral boundary and lower boundary NCEP reanalysis (Kalnay et al. 1996) data and Reynolds weekly sea surface temperature (SST) (Reynolds et al. 2002), respectively, are used to force the model. Control simulations of about 27 years (01-11-1981 to 31-12-2008) are carried out to validate the model climatology. Control run is initialized once at the beginning (00GMT 01-11-1981) and then continued up to the end of December 2008. In order to test our hypothesis, we have used two sets of boundary forcing (1982, 1989) for two separate simulations each for 31 years. At a time one of these boundary conditions is used year after year successively to get one set of simulation. The year 1982 (1989) was drought (normal) and El Niño (non-ENSO) year. Though there is no established link between pre-onset rainfall variability and the large scale external influences like ENSO, the choice of such two different boundary conditions is expected to shed light on the statistics of the ‘internal’ IAV generated due to external influences (if any). In principle, any boundary conditions which produce sufficiently large interannual pre-onset rainfall variability over CI can be used to test the hypothesis. The model is initialized with the boundary condition of 00GMT 1st January and for the successive runs, restart files of preceding run are used. In our study we have used data of May–September months only. Therefore, the first 6 and 4 months of the control and FBC runs, respectively, are automatically discarded from our analysis with no further simulations being discarded as spinup. This setup allows the slowly varying field such as soil moisture to evolve and carry information from one year to another. Hereafter these simulations

will be referred to as fixed boundary condition (FBC) run. The primary conditions to prove this hypothesis are: (a) there should be large pre-onset monsoon rainfall variability over CI, (b) monsoon simulation should be reasonably realistic in the model.

3 Observed data and methodology

Asian precipitation-highly resolved observational data integration towards evaluation (APHRODITE) water resources rainfall data (0.5° × 0.5°) for the year 1980–2002 (<http://www.chikyu.ac.jp/precip/index.html>) and India Meteorological Department (IMD) generated gridded (1° × 1°) daily rainfall data (1951–2007) (Rajeevan et al. 2006) are used to validate the model rainfall over land. GPCP (Adler et al. 2003) pentad rainfall data for the period 1979–2008 are used to validate the large scale rainfall pattern in the model.

Central India (75.30°–86.63°E, 16.92°–26.43°N) represents a homogeneous summer monsoon rainfall region and hence the average rainfall over this region can be used for the monsoon climate study (Goswami et al. 2006). The observed pre-onset rainfall (CI averaged) shows large IAV with mean and interannual variance of 12.82 and 109.99 mm², respectively. Here pre-onset rainfall is taken as accumulated rainfall in the past 15 days from the onset date over Kerala (defined by IMD). The year to year variation of accumulated pre-onset rainfall is within the range of 0.94–76.82 mm. Since the monsoon rainfall covers whole CI after about 2 weeks from the onset date (over Kerala), the accumulated rainfall considered here represents rainfall of previous 3–4 weeks from the actual onset date over CI. Due to very hot and dry summer conditions, it is also expected that the soil moisture will lose its memory of any rainfall event which may have occurred sufficiently prior to the onset date. Furthermore, if we consider the accumulated rainfall of past one month instead of 15 days, the statistics also does not change much. Therefore, accumulated rainfall over CI during 15 days time length prior to the onset over Kerala may be defined as pre-onset rainfall.

The monthly composites of ‘internal’ rainfall (Fig. 1) are calculated using gridded daily rainfall data (1951–2007) from IMD in the following steps: (a) daily rainfall anomalies are created by removing the first four Fourier harmonics (a smoothed annual variation) from the daily rainfall data. This method is often used for calculating daily anomaly (e.g. Wang and Xu 1997; Ajayamohan and Goswami 2003), (b) monthly anomalies are created by averaging daily anomalies and then, these 57 years of monthly anomalies are used to create monthly composite. Following Xavier et al. (2007), the north–south tropospheric temperature gradient (TTG) is calculated using

vertically averaged (200–600 hPa) temperature difference between a northern box (40.2–100°E, 5–35°N) and southern box (40.2–100°E, 10°S–5°N). Since the southern limit of model domain is 10.8°S, we use southern box starting from 10°S, instead of 15°S as used in Xavier et al. (2007).

The pre-onset rainfall and its interactions with the first phase of CISO through variation in soil moisture are considered here as ‘internal’ to the monsoon system rather than simply land–atmosphere interaction. In general, the variation of soil moisture takes place on monthly to seasonal time scale and its interaction with atmosphere is considered as external influence. However, in the present context the pre-onset rainfall is quite unpredictable and the time scale of possible interactions with the first phase of CISO is short. The mean and interannual standard deviation of pre-onset rainfall are also in the same order and cannot be predicted. Therefore, the pre-onset soil moisture variability and its

interaction with CISO may be considered as ‘internal’ influence.

4 Control simulation

In the past, many studies have been carried out to simulate the Indian monsoon using RCM (e.g. Bhaskaran et al. 1996; Ratnam and Kumar 2005; Dash et al. 2006; Chow et al. 2006; Ratnam et al. 2009; Ashfaq et al. 2009). However, most of those studies used few years of model simulation. Here we investigate the mean and variability of monsoon climate using 27 years of control simulation by RegCM3. Figure 3d–f shows the JJAS averaged (1982–2008) rainfall from IMD, APHRODITE and RegCM3, respectively. The model is able to capture the rainfall maxima regions of western-ghat, central and north-

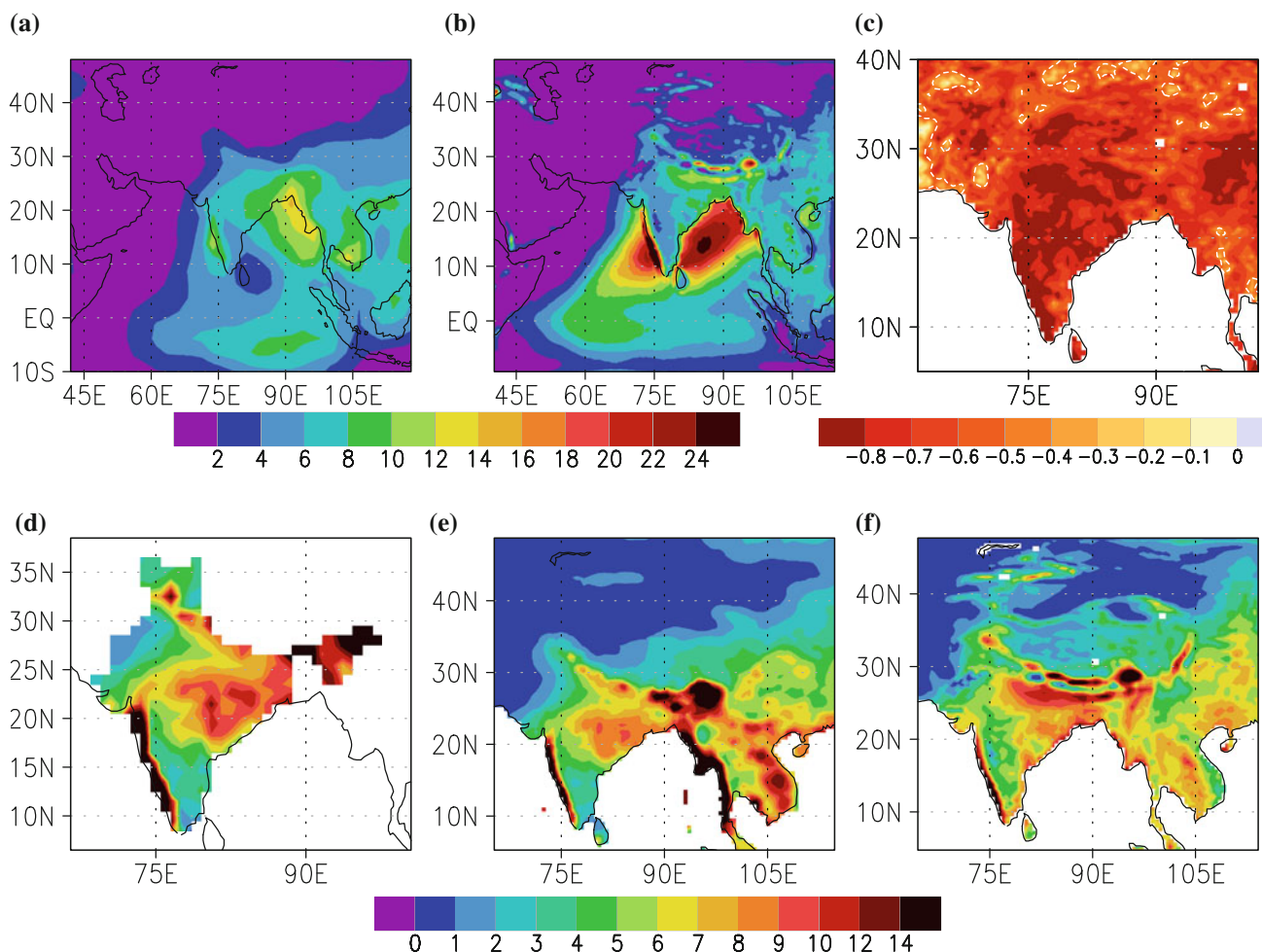


Fig. 3 a Seasonal (JJAS) averaged GPCP rainfall in mm day^{-1} (1979–2008). b JJAS averaged rainfall (mm day^{-1}) in RegCM3 control simulation (1982–2008) for the whole domain. c Correlation between May and June ‘internal’ rainfall based on RegCM3 control simulation (1982–2008). d JJAS averaged rainfall (mm day^{-1}) based

on IMD gridded data (1951–2007). e JJAS averaged rainfall (mm day^{-1}) from APHRODITE (Asian precipitation-highly resolved observational data integration towards evaluation) water resources rainfall (1980–2002). f JJAS averaged rainfall (mm day^{-1}) in RegCM3 control simulation (land part only)

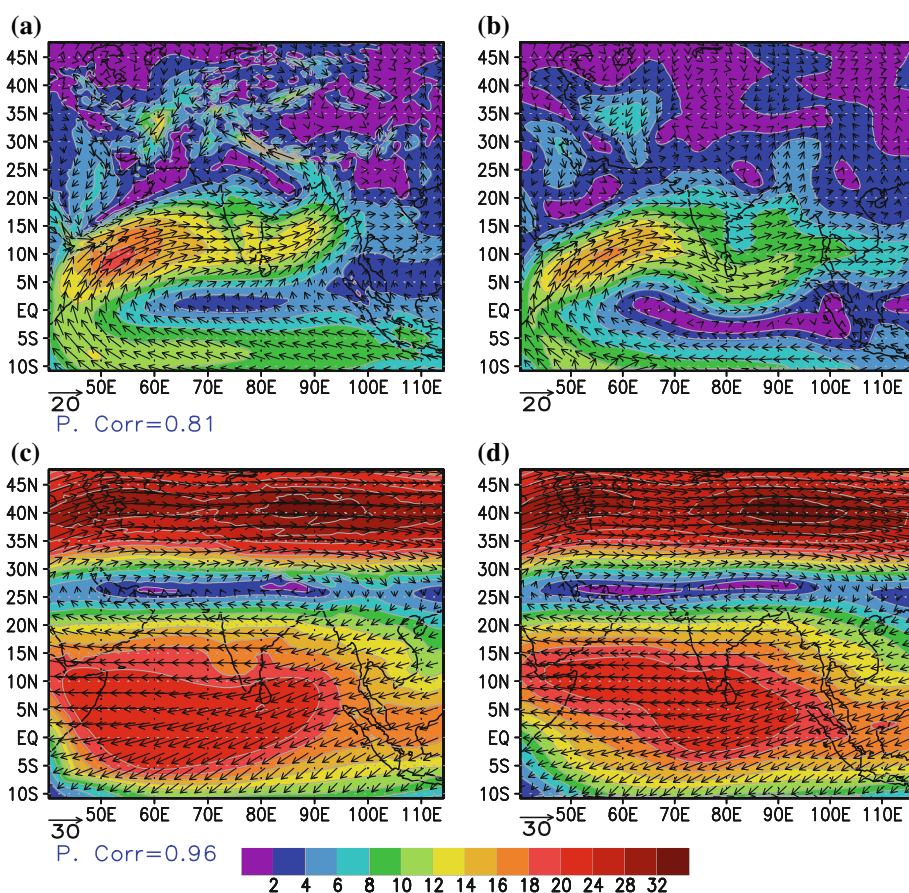
east India and foothill of Himalayan region. The pattern correlation between model and APHRODITE rainfall is 0.73 over the model domain. Furthermore, correlation between May and June ‘internal’ rainfall (Fig. 3c) reveals the fact which is similar to the observation where the May and June rainfall are inversely correlated. In general, the rainfall pattern simulated by the model over land is quite good compared to the observations. However, the model overestimates rainfall over south-east Arabian sea and north Bay of Bengal as compared to GPCP (Fig. 3a, b), which is similar as shown by Ratnam et al. (2009). Also the equatorial maxima rainfall region is shifted towards east. This rainfall bias has been shown to be linked with the lack of ocean–atmosphere coupling (Ratnam et al. 2009) and the choice of convective parameterizations (Chow et al. 2006) in RegCM3. In a coupled ocean–atmosphere system, the warmer SST supports the convection and convection brings rainfall which eventually cools the SST. Since the SST in RegCM3 is prescribed, above feedback is absent. Therefore the warmer SST continuously supports the convection despite heavy rainfall and this may enhance the rainfall in the model.

The locations of low level jet over Arabian sea, cross equatorial flow and the easterly wind at the south of

equator are well captured by the model (Fig. 4). However, the wind speed is slightly stronger, which is consistent with the rainfall bias over ocean. The pattern correlation between simulated wind and the NCEP reanalysis at 850 hPa is 0.85. The strength of upper level (200 hPa) westerly Jet at about north of 30°N and easterly Jet over equatorial Indian Ocean are also well captured by the model. The pattern correlation between model simulated and NCEP reanalysis wind at 200 hPa is 0.96.

The ability of RegCM3 to simulate the evolution of Indian summer monsoon can be examined by analyzing the time evolution of kinetic energy (KE) of low level wind over Arabian Sea and the time evolution of rainfall as a function of latitude (Goswami and Xavier 2005). In a recent study, the strength of zonal wind over southern Arabian Sea has been used as an index to define the onset date of monsoon (Wang et al. 2009). According to definition of Wang et al. (2009) (Wang index), the onset date is the first day of the period when area averaged (5°–15°N, 40°–80°E) zonal wind continuously exceeds 6.2 m s^{-2} for more than 7 days (including the onset day). The basic idea behind such a choice is that the onset of Indian summer monsoon is linked with the rapid increase of low level wind. At the same time the tropical convergence zone moves towards the north, over Indian

Fig. 4 JJAS averaged wind at 850 and 200 hPa levels from NCEP reanalysis and RegCM3 control simulation. **a** RegCM3 at 850 hPa, **b** NCEP reanalysis at 850 hPa, **c** RegCM3 at 200 hPa, **d** NCEP at 200 hPa. The *color shading* represent the magnitude of wind (m s^{-1}) and *arrow* represent the wind direction



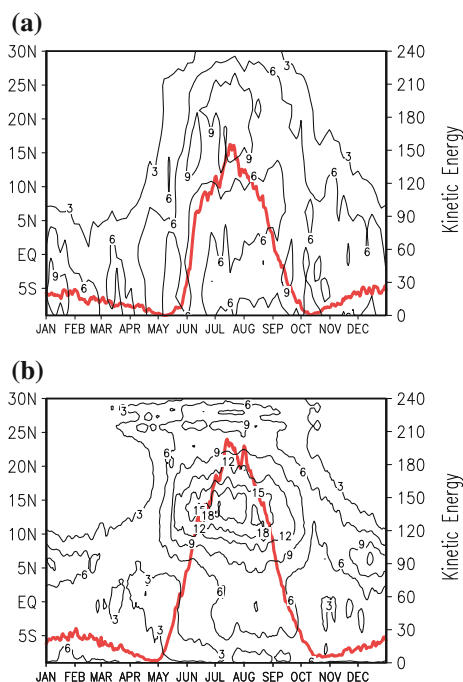


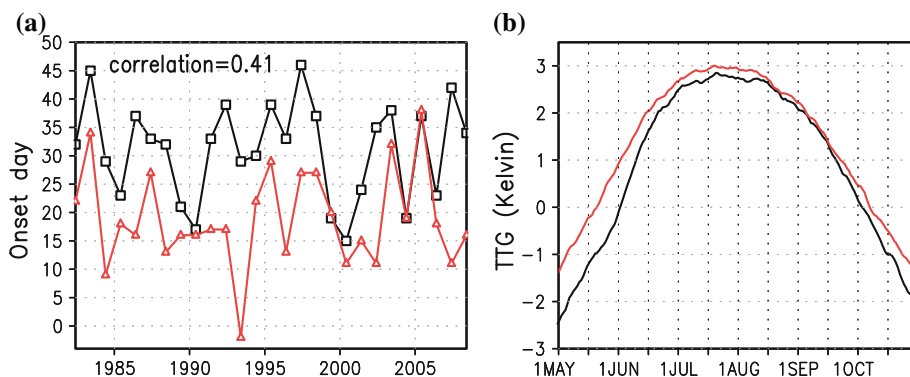
Fig. 5 Temporal evolution of 70°–100°E averaged rainfall (mm day^{-1}) as a function of latitude (*thin black contour*). Kinetic energy ($\text{m}^2 \text{s}^{-2}$) at 850 hPa of daily climatology wind, averaged over 50°–65°E, 5°–15°N are represented by *red and thick line* in each panel with scale on the *right*. **a** GPCP rainfall and NCEP wind, **b** RegCM3 control

subcontinent. Therefore, area averaged winds over a box (50°–65°E, 5°–15°N) as defined by Goswami and Xavier (2005) are used to calculate KE. A sharp increase in KE around 1st June (Fig. 5a) is seen in NCEP reanalysis data and that date happens to be the climatological summer monsoon onset date over Kerala. The KE on 1st June using NCEP (RegCM3) data is 31.6 (83.7) $\text{m}^2 \text{s}^{-2}$. Thin contour in Fig. 5a, b shows the daily climatology rainfall, averaged over 70°–100°E as a function of latitude. Both, the model and GPCP data show a preferred location of maximum rainfall at around 15°N during the month June–September. However, the model rainfall is twice that of observation (GPCP) and it

is primarily due to the excessive rainfall over oceanic region. Based on Wang index, the monsoon onset in the model is advanced as compared to the NCEP reanalysis data (Fig. 6a). The correlation between the time series of model and NCEP onset dates is 0.41 and the climatological onset day in NCEP (RegCM3) is 31.40 (19.22) with interannual standard deviation of 8.30 (8.31) days. Here 1st May is counted as day 1. The north–south TTG over Indian monsoon region is also closely linked with the onset and withdrawal date (e.g. Xavier et al. 2007). The early positive reversal of TTG in the model (Fig. 6b) is associated with the early onset. During post-onset time the TTG in the model is also higher than that of NCEP. The systematic rainfall bias over Arabian Sea and Bay of Bengal may be linked with the enhanced TTG in the model. Using Xavier et al. (2007) criteria of onset (TTG index), the climatological onset day in NCEP (RegCM3) is 31.59 (19.59) with interannual standard deviation of 7.65 (7.56) days. Though the model is able to capture the IAV of Indian summer monsoon onset day, the climatological onset takes place in advance by about 10 days.

Since the calculated onset statistics using the methods of Wang et al. (2009) and Xavier et al. (2007) are very similar to each other, any one of them can be used for defining the onset date. The large-scale model simulated pre-onset (15 days average before the onset date) and JJAS averaged 2m air temperatures are reasonable as compared to the NCEP reanalysis (Fig. 7). Here onset dates defined by TTG index are used. The pattern correlation between NCEP and RegCM3 pre-onset and JJAS 2m air temperature are 0.96 and 0.95, respectively. Though the JJAS averaged model rainfall over India is reasonably realistic, it has cold bias in the 2m air temperature by about 3°C. The cold bias is probably linked with the land-surface schemes in the model and also some of the differences are due to different horizontal resolution of the model and NCEP reanalysis data. The pre-onset land–ocean temperature gradient is about 5°C in both NCEP and RegCM3, while the land–ocean temperature gradient is almost disappeared during the monsoon season (JJAS averaged).

Fig. 6 a Onset dates [based on Wang et al. (2009) criteria] using NCEP reanalysis data (*black*) and RegCM3 control simulation (*red*). The onset dates are counted from 1st May (1st May = 01, ..., 1st June = 32, ...). **b** Daily climatological mean (1982–2008) tropospheric temperature gradient using NCEP (*black*) and RegCM3 control simulation (*red*)



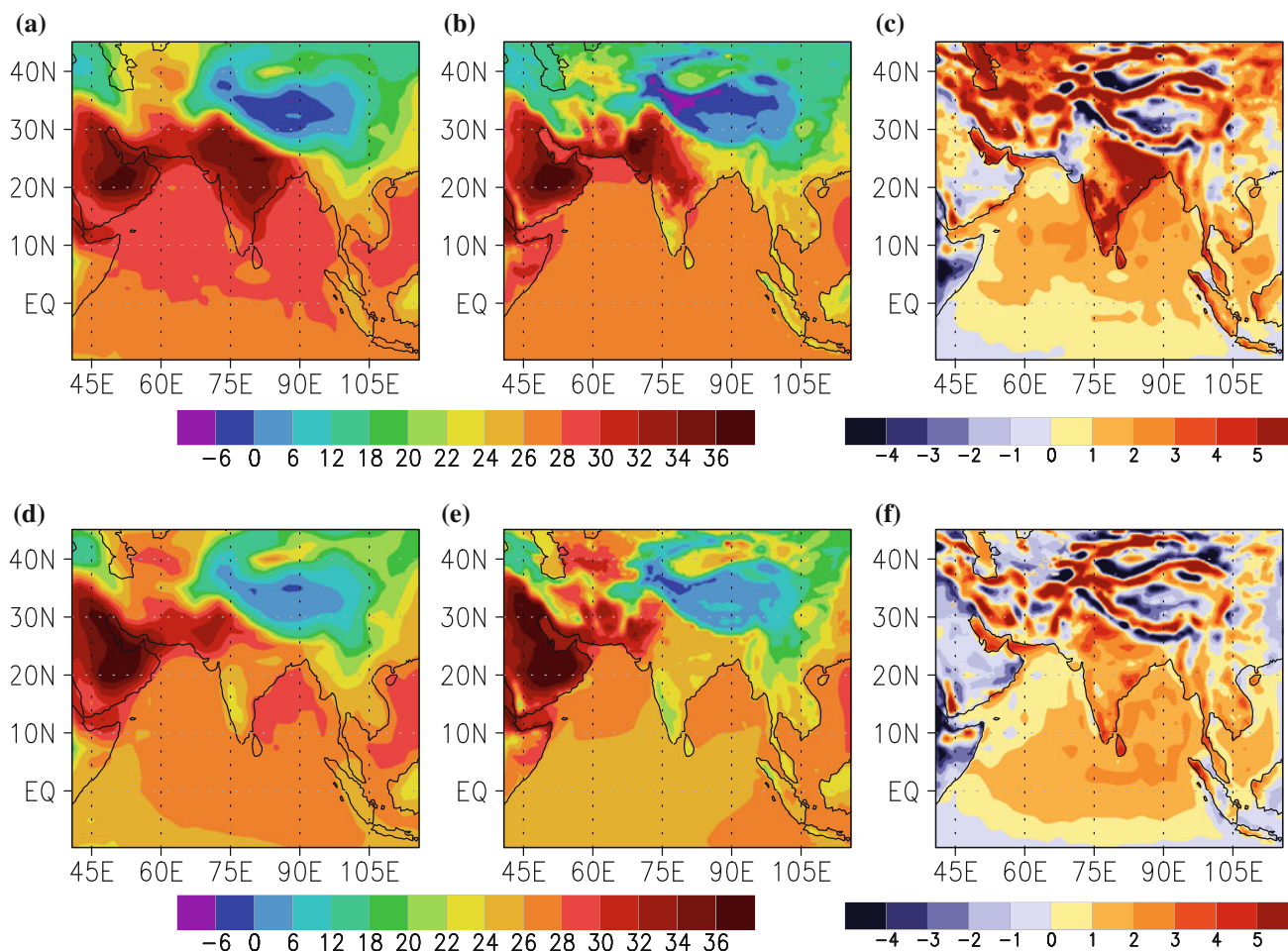


Fig. 7 Pre-onset (15 days average prior to the onset date) and JJAS averaged 2 m/near-surface air temperature (1982–2008) in °C. **a** Pre-onset NCEP, **b** pre-onset RegCM3 control simulation, **c**

difference between NCEP and RegCM3 (**a, b**) pre-onset temperature, **d** JJAS averaged NCEP, **e** JJAS averaged RegCM3 control simulation, **f** difference between NCEP and RegCM3 (**d, e**)

Lead/lag regressed rainfall anomaly, averaged over 70°–90°E as a function of latitude from GPCP and RegCM3 are shown in Fig. 8a, b, respectively. Rainfall anomalies are calculated by removing first 4 harmonics and retaining periodicity between 20 and 100 days by using Lanczos filter (Duchon 1979). The reference time series for regression is computed based on the averaged filtered precipitation anomalies over a box (12°–22°N, 70°–95°E) in the primary zone of maximum rainfall. The northward propagation of rainfall anomaly or ISO, which starts at about 10°S and ends at around 25°N is also seen in the model. Though the primary rainfall maxima is captured by the model, the secondary maxima situated about south of the equator is not captured well. The phase-speed of northward propagating ISO can be estimated from Fig. 8. In GPCP data, the phase speed of ISO is about 1° day⁻¹ and in RegCM the phase speed between equator and 15°N is about 0.75° day⁻¹. Beyond 15°N, the phase speed is about 1.34° day⁻¹. Since the southern boundary of model

domain is around 10°S, the ISO variability south of equator is constrained by the boundary forcing. A very distinct and continuous northward propagation of ISO is evident in some particular years of RegCM3 simulation. Year 1983 is one of them where, continuous propagation of rainfall anomaly starting from equator to 25°N is seen (Fig. 8c).

5 Fixed boundary condition simulation

The motivation behind the FBC run is to quantify the interannual monsoon variability generated by the internal feedback within this region and to identify the possible reasons. If there is large pre-onset rainfall in the control simulation of a particular year, the boundary condition of that particular year may produce significant pre-onset rainfall in each and every year of FBC run. The large-scale events, like high rainfall during pre-onset time over CI may be due to the boundary forcing. Furthermore, IAV in the

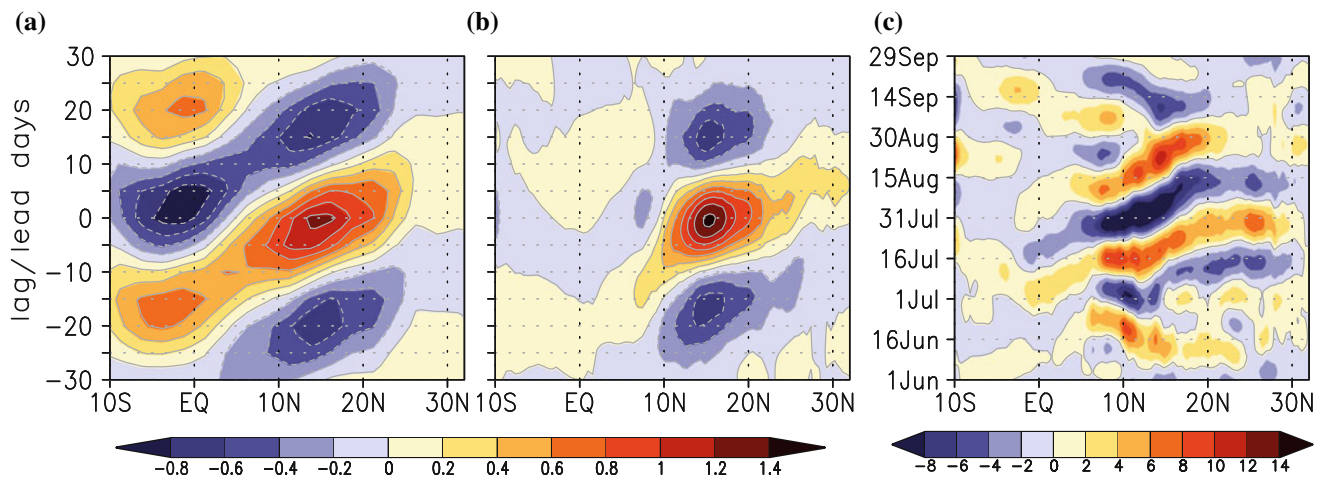


Fig. 8 Regressed anomalies (20–100 filtered) of rainfall (mm day^{-1}) averaged over 70° – 90°E as a function of latitude and lead/lag days **a** from GPCP, **b** from RegCM3 control. Contour interval is 0.2.

c Hovmöller diagram of 20–100 days filtered rainfall anomaly (mm day^{-1}) averaged over 70° – 90°E for the year 1983 from RegCM3 control simulation

pre-onset rainfall due to nonlinear land–atmosphere feedback is also expected in the FBC run. Thus choice of such boundary condition for FBC run will shed light on the monsoon ‘internal’ IAV, generated due to pre-onset land-surface condition. Since, CI is the representative area for monsoon climate, the summer monsoon rainfall statistics over this region are calculated to compare the FBC runs with the control simulation. Here we have used first 27 years of FBC simulations for the comparison of statistics with the control simulation. The climatological onset date in FBC 1982 and FBC 1989 runs, using Wang index (TTG index) are 27.37 and 14.25 (31.19 and 17.67), respectively, with interannual standard deviation of 2.58 and 1.23 (0.59 and 0.53) days, respectively. The onset date in the NCEP reanalysis for the years 1982, 1989 are 32 and 21, respectively. Therefore, the onset dates in both FBC runs are advanced by maxima of 5–7 days, which are within the range of mean onset bias in the control simulation. Using Wang index (TTG index) the accumulated pre-onset rainfall over CI for FBC 1982 and 1989 are 74.76 and 20.87 mm (63.94 and 25.27 mm), respectively, and the respective interannual variances are 55.89 and 7.51 mm^2 (44.94 and 14.92 mm^2). The pre-onset rainfall over CI is primarily due to the non-monsoon convective activity and there is little possibility that it is mixed with onset or post-onset monsoon rainfall because the monsoon rainfall over CI starts later than the onset date used here (onset date over Kerala).

Since the boundary forcing remains same for each year, the IAV generated in ‘internal’ simulation using a RCM will be less compared to that of global atmospheric general circulation model (e.g. Krishnan et al. 2009). Figure 9 shows the normalized seasonal (JJAS) rainfall anomaly in the FBC runs over CI. The FBC 1982 and 1989 runs show

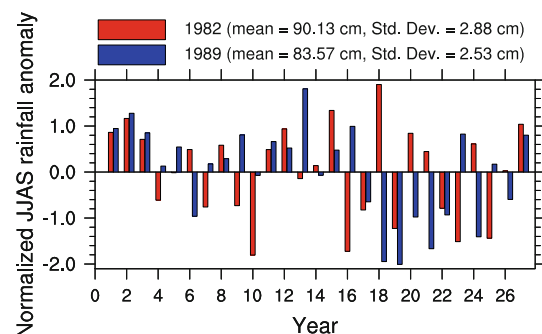


Fig. 9 Normalized seasonal (JJAS) rainfall anomaly (cm) over CI from FBC 1982 (red) and FBC 1989 (blue) runs. The deviations of CI averaged JJAS rainfall from 27 years mean have been normalized by interannual standard deviation

seasonal mean rainfall of 90.13 and 83.57 cm with inter-annual standard deviation of 2.88 and 2.53 cm, respectively. The CI averaged mean rainfall in the control simulation is 86.24 cm with standard deviation of 8.08 cm. Therefore, the IAV of rainfall in FBC 1981 and 1989 runs are about 35 and 31% of control simulation. In principle, one-way nesting of RCM restricts the modulation of large-scale component of monsoon circulation. Otherwise it will modulate the circulation of the scale larger than the current model domain and probably, that would generate more ‘internal’ IAV. Furthermore, above two FBC runs show that, it is primarily the boundary conditions which generate large pre-onset rainfall over CI.

Where does the ‘internal’ IAV arise from in the model simulation? Is this variability related to the land–atmosphere feedback around onset time? To answer these questions we have calculated interannual standard deviation of monthly rainfall for the months June–September. If the IAV of seasonal rainfall is due to noise, the interannual

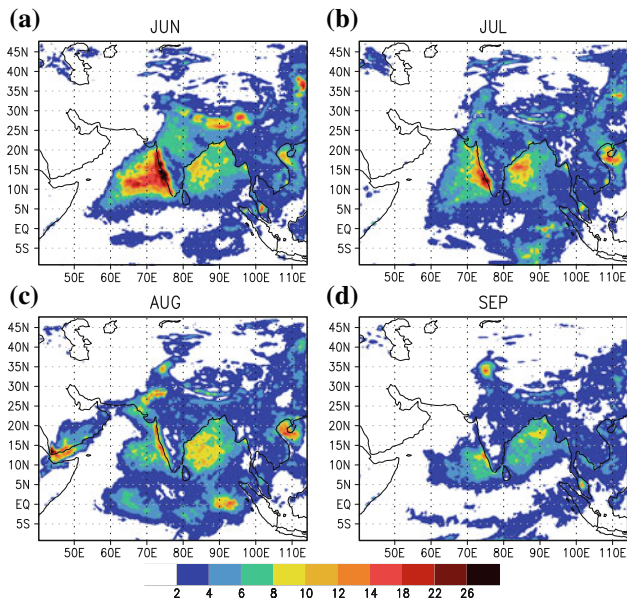


Fig. 10 Interannual standard deviation of accumulated monthly rainfall (cm) from FBC 1982 simulation

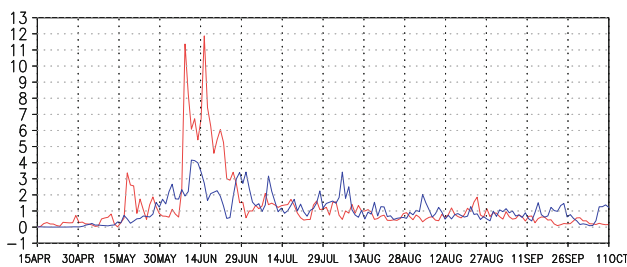


Fig. 11 Interannual variance of CI averaged rainfall ($\text{mm}^2 \text{day}^{-2}$) in FBC 1982 (red) and FBC 1989 (blue) simulations

monthly variability will be evenly distributed in all four months. It turns out that the month June produces largest IAV (Fig. 10) over CI as well as over coastal part of Arabian Sea. The interannual variance of CI averaged daily rainfall shows the largest variability during the month June (Fig. 11) and the maximum values for FBC 1982 and 1989 are ≈ 11 and $\approx 4 \text{ mm}^2 \text{day}^{-2}$, respectively. Therefore, the IAV in the model is not totally due to climate noise, but there are some systematic variations and that is large in June. Furthermore, a relatively larger pre-onset rainfall variability around 17th May in FBC 1982 run is followed by very large rainfall variability around middle of June. The largest June rainfall variability clearly indicates a link with the pre-onset rainfall, through ‘internal’ land–atmosphere feedback. On the other hand, the FBC 1989 run shows larger rainfall variability compared to FBC 1982 during July–September. Though the July–September rainfall variability are smaller, their contribution towards the interannual variability in FBC 1989 run cannot be

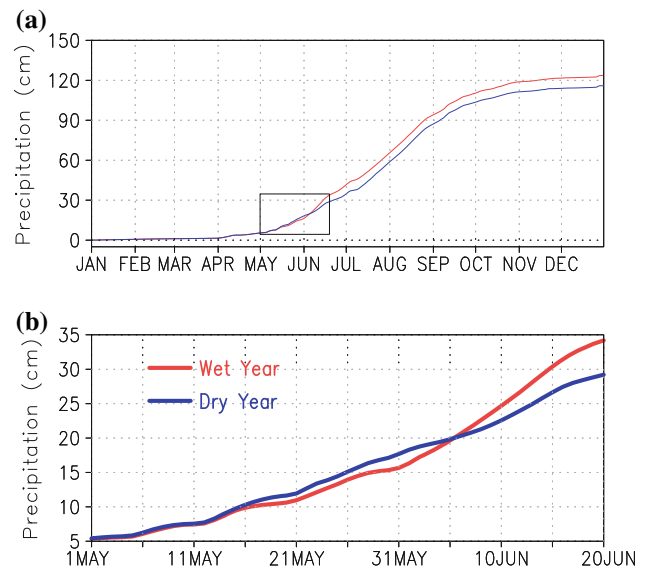


Fig. 12 a Time evolution of CI averaged accumulated rainfall in cm (FBC 1982). Wet and dry year composites are shown in red and blue color, respectively. b Magnified view of box in a

neglected (CI averaged rainfall standard deviation in FBC 1982, 1989 are of same order). Since the pre-onset rainfall variability in FBC 1989 run is very small, it cannot be used for testing the hypothesis. Therefore, we present here the detail analysis of FBC 1982 run. To gain further insight, out of 31 years of FBC 1982 run, we have identified 6 years as excess rainfall years (≥ 0.9 standard deviation) and another 6 years as deficit rainfall years (≤ -0.9 standard deviation). Hereafter the excess and deficit rainfall years will be referred as ‘wet’ and ‘dry’ years, respectively. Here, the meaning of ‘wet’ and ‘dry’ years are different from the actual definition of Indian summer monsoon dry and wet years. The former is based on ‘internal’ model simulation where interannual standard deviation of rainfall is about 30% of observations.

We have created a time series of CI averaged accumulated rainfall (land part only) for all ‘wet’ and ‘dry’ years. Figure 12 shows the composite of ‘wet’ and ‘dry’ year accumulated rainfall. Above (below) normal rainfall in May decreases (increases) the rainfall in June and beyond June, the two composites are almost parallel. Therefore, the largest IAV in June rainfall (Fig. 10) is arising primarily due to internally generated pre-onset land-surface conditions and that variability (i.e. June rainfall) determines whether a year is going to be ‘wet’ or ‘dry’. Pre-onset to onset phase of monsoon is unstable and weak compared to its mature phase. Therefore in that phase, the monsoon can get perturbed easily due to the feedback arising from land–atmosphere interactions. Model indeed shows largest variability during transition period.

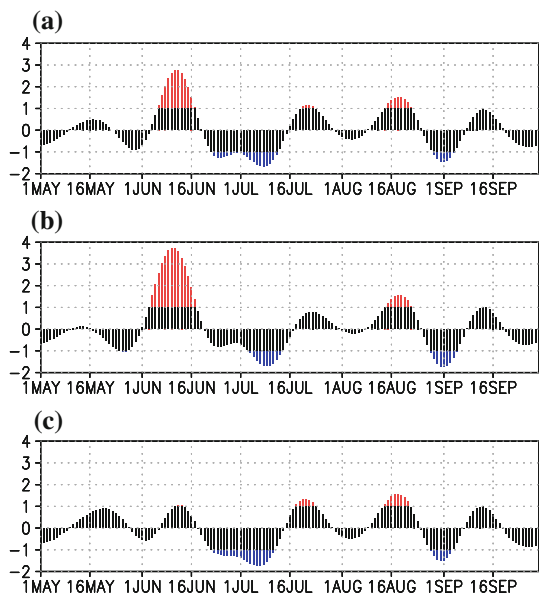


Fig. 13 CI averaged 20–100 days filtered rainfall anomaly (mm day^{-1}) from FBC 1982 run (normalized by their own standard deviation). **a** Composite of all years (31 years). **b** Composite of wet years. **c** Composite of dry years

However, from the above it is not clear whether the CISO has been modulated. We will now examine if there was any modulation of CISO, particularly during “wet” and “dry” years. To do so, time series of 20–100 days filtered rainfall anomaly, averaged over CI land part has been constructed for all 31 years. Figure 13a shows the composite of 31 years normalized (by May–September rainfall standard deviation) rainfall anomaly from 1st May to 30th September. This composite shows nothing but the CISO. The planetary scale background condition of 1982 has produced three active and two break events. Here active (break) condition is identified when the anomalous rainfall is greater (less) than or equal to $+1$ (-1) standard deviation. Similarly, the composite of rainfall anomalies for “wet” and “dry” years are shown in Fig. 13b, c, respectively. Major changes in phase as well as in the amplitude of CISO are seen between middle of May to end of June. Other than this period, phase and amplitude of CISO in Fig. 13a–c are very similar to each other. During “wet” years, a negative rainfall anomaly is appeared between 17th and 31st May followed by an enhanced active condition for 15 days. On the other hand, during “dry” years, an anomalous positive rainfall is appeared between 10th and 27th May, followed by a much weaker positive anomaly.

Pre-monsoon land–ocean temperature gradient primarily drives the low-level moist wind into the continent and initiates the monsoon circulation. A notable change in pre-onset low-level moisture convergence is also seen between “dry” and “wet” years (Fig. 14). These changes are due to

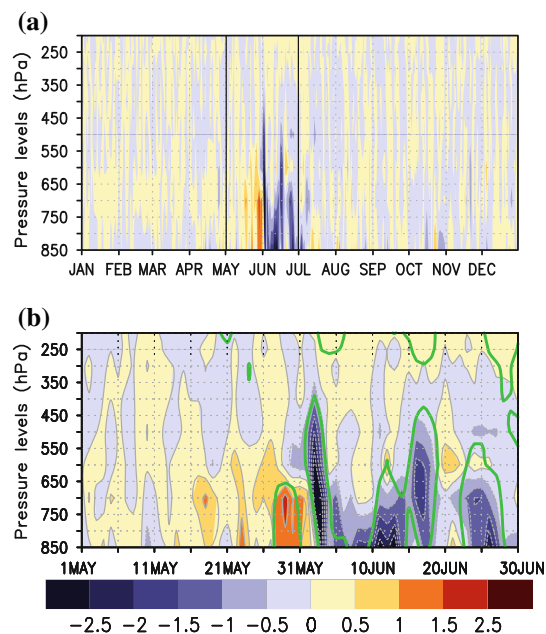


Fig. 14 **a** Difference between “wet” and “dry” year composites (wet–dry) of CI averaged moisture convergence ($\nabla \cdot qU$; $10^{-8} \text{ kg kg}^{-1} \text{ s}^{-1}$) from FBC 1982 run. **b** Magnified view of **a** for the time period 1 May to 30 June. Green contours show 95% significance level

unpredictable internal dynamics. An increase (decrease) in low level moisture convergence during pre-onset condition vigorously decreases (increases) the moisture convergence (significant at 95% level) during the onset phase. It may be noted (Fig. 14) that, moisture convergence is largely confined to the lower layers.

The surface temperature and soil moisture condition before and after the onset are examined in Fig. 15. The CI averaged difference in 2m air temperature between “dry” and “wet” years changes sign within 1–2st June (Fig. 15c). Pre-onset 2m air temperature is warmer (colder) during the “wet” (“dry”) years and the vice versa. Naturally, the warmer (colder) pre-onset 2m air temperature is due to decrease (increase) in pre-onset rainfall, which is evident from the surface soil moisture (Fig. 15a). The color shaded area in Fig. 15a, c are significant at 95% level. Using onset date of individual years (defined by TTG index), 15 days averaged (prior to onset) soil moisture and 2m air temperature are calculated to examine the spatial distribution of pre-onset “wet” and “dry” years land-surface conditions. The CI averaged total pre-onset and June–September monthly rainfall during “wet”, “dry” and all 31 years are summarized in Table 1. The differences between “wet” and “dry” years accumulated rainfall during pre-onset and during the month of June are 9.50 and 87.57 mm, respectively. Other months (July–September) do not show significant difference in accumulated rainfall among “wet”, “dry” and all years average. The average pre-onset surface

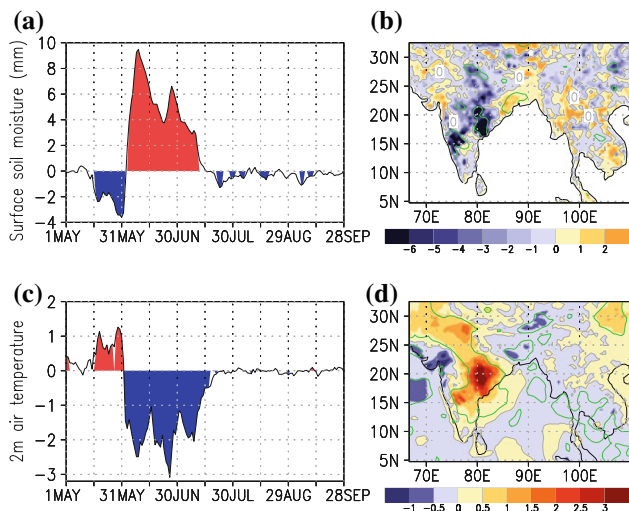


Fig. 15 Difference between “wet” and “dry” year composite (wet–dry) of 2m air temperature and surface (10 cm) soil moisture in FBC 1982 run. **a** CI averaged soil moisture (mm), **c** CI averaged 2m air temperature (°C). *Color shaded* region are significant at 95% level. Difference in pre-onset (15 days average prior to the onset date) composite of **b** surface soil moisture (mm), **d** 2m air temperature (°C). The *green contour* represents the 95% significance level

Table 1 CI averaged total rainfall composite for “wet”, “dry” and all 31 years during pre-onset (15 days), June, July, August and September

	Pre-onset	June	July	August	September
All year	42.97	204.25	241.56	289.52	166.65
“Wet” year	39.49	250.05	241.93	287.96	164.57
“Dry” year	48.99	162.48	240.49	287.24	166.43

Onset dates are defined using TTG index

temperature is significantly (95% significance level) warmer during “wet” year compared to “dry” year over large part of the CI with maximum of 3°C (Fig. 15d). A relatively dry pre-onset land-surface condition (Fig. 15b) during “wet” years is also consistent with the decrease in pre-onset rainfall. Therefore, the pre-onset land–ocean temperature gradient is relatively larger during the “wet” years compared to “dry” years and that leads to enhanced low level moisture convergence. A strong moisture convergence leads to an anomalous cooling in the surface and produces anomalous dry condition. This anomalous dry condition creates a favourable condition for convection and hence moisture convergence increases. The net moisture convergence (or rain) during June is high (low) due to low moisture convergence during pre-onset time. Therefore, though the pre-onset conditions are not predictable, there is certain predictability of June rainfall based on pre-onset condition.

6 Conclusions

Long control simulations (27 years) are carried out using regional climate model RegCM3 to investigate the monsoonal climate in the model. Though the seasonal rainfall (JJAS averaged) over Arabian Sea and Bay of Bengal is overestimated, the model is able to capture the rainfall pattern over land part quite well. The location of low level and upper level monsoon Jets and their magnitude are also nicely reproduced. On the intraseasonal time scale, the simulated northward propagation of ISO is reasonably good in the model. The IAV of CI rainfall and onset date in the control simulation of RegCM3 are close to the observations.

Understanding the mechanism of ‘internal’ IAV is the key towards improving seasonal prediction of Indian summer monsoon. Here we have proposed that the pre-onset land–atmosphere interaction can give rise to ‘internal’ IAV through the modulation of CISO. Observations indeed show that increase in ‘internal’ May rainfall is followed by a decrease in June rainfall and the vice versa. To test our hypothesis we have used the RCM RegCM3, successively forced with two different boundary condition (1982, 1989) in two separate simulations each for 31 years (FBC runs) over the Indian monsoon region. Hence the IAV generated in the model is not connected with the IAV of external influences but, mainly due to the internal land–atmosphere feedback.

Using FBC 1982 run, it has been shown that the land–atmosphere interaction modulates the phase and amplitude of CISO during the months May–June. A dry (wet) pre-onset (May) land-surface condition increases (decreases) rainfall in June while the remaining months of the season do not show much change. The June anomaly leads to an anomalous change in seasonal rainfall. Thus, the IAV of seasonal rainfall is connected with the pre-onset land-surface condition which is unpredictable and generates internally. Though the pre-onset rainfall spells are unpredictable, it plays a deterministic role on the anomalous seasonal rainfall and can be used for improving the forecasts within the season.

While the IAV of seasonal rainfall in FBC 1982 and 1989 runs are of the same order, the mean and interannual variability of pre-onset rainfall in the FBC 1989 run are very small. Therefore, the impact of pre-onset rainfall on the first phase of CISO could not be seen very clearly. Hence, the generation of ‘internal’ summer monsoon rainfall variability may not be related with the external influences. However, the interannual rainfall variability in FBC 1989 run is relatively larger during the months July–September. Probably the variability in land-surface conditions during monsoon season also contributes to the ‘internal’ variability. The ISO may interact with the prevailing land-surface

conditions and create certain rainfall changes within the monsoon season. Observational and modeling study in the past have shown strong negative correlation between soil moisture and rainfall at 10–15 days lag. The memory of past rainfall during ISO active phase may prevail in the soil and interact with the next active phase of ISO. Therefore, it will be interesting to investigate whether the 'internal' variability particularly in FBC 1989 run are generated due to the interactions between 10 and 20 days mode of ISO and the land-surface processes.

Though a large amplitude of pre-onset rainfall is the necessary condition for proving our hypothesis, this study could not bring out appropriate methods of boundary condition selection. Thus, the choice of boundary conditions remains trivial. Furthermore, the strength of land–atmosphere coupling are different in different model. Therefore, similar experiments with other climate model may also increase our confidence in this finding.

This is the first time that a clear link between pre-onset and seasonal monsoon rainfall variability is demonstrated using a RCM. Our result suggests that the initialization of soil moisture with realistic data may improve the seasonal forecast of Indian summer monsoon rainfall.

Acknowledgments We thank Abdus Salam International Centre for Theoretical Physics in Trieste, Italy for making available the model codes of RegCM3 for this study. IITM is supported by Ministry of Earth Sciences, Government of India, New Delhi. Fellowship of S. Halder is sponsored by CSIR. We thank two anonymous reviewers for their constructive comments to improve the earlier version of this manuscript.

References

- Adler RF, Huffman GJ, Chang A, Ferraro R, Xie P, Janowiak J, Rudolf B, Schneider U, Curtis S, Bolvin D, Gruber A, Susskind J, Arkin P (2003) The version 2 global precipitation climatology project (GPCP) monthly precipitation analysis (1979–present). *J Hydrometeorol* 4:1147–1167
- Ajayamohan RS, Goswami BN (2003) Potential predictability of the Asian summer monsoon on monthly and seasonal time scales. *Meteorol Atmos Phys*. doi:10.1007/s00703-002-0576-4
- Ashfaq M, Shi Y, Tung W-w, Trapp RJ, Gao X, Pal JS, Diffenbaugh NS (2009) Suppression of south Asian summer monsoon precipitation in the 21st century. *Geophys Res Lett* 36:L01704. doi:10.1029/2008GL036500
- Bhaskaran B, Jones RG, Murphy JM, Noguera M (1996) Simulations of the Indian summer monsoon using a nested climate model: domain size experiments. *Clim Dyn* 12:573–587
- Chow KC, Chan JCL, Pal JS, Giorgi F (2006) Convection suppression criteria applied to the MIT cumulus parameterization scheme for simulating the Asian summer monsoon. *Geophys Res Lett* 33:L24709. doi:10.1029/2006GL028026
- Dash SK, Shekhar MS, Singh GP (2006) Simulation of Indian summer monsoon circulation and rainfall using RegCM3. *Theor Appl Climatol* 86:161–172
- Dickinson RE, Henderson-Sellers A, Kennedy PJ (1993) Biosphere–atmosphere transfer scheme (BATS) version 1e as coupled to the NCAR community climate model, NCAR Technical Note NCAR/TN-387+STR, National Center for Atmospheric Research, Boulder, CO
- Duchon CE (1979) Lanczos filtering on one and two dimensions. *J Appl Meteorol* 18:1016–1022
- Fritsch JM, and Chappell CF (1980) Numerical prediction of convectively driven mesoscale pressure systems. Part I: convective parameterization. *J Atmos Sci* 37:1722–1733
- Goswami BN, Venugopal V, Sengupta D, Madhusoodanan MS, Xavier PK (2006) Increasing trend of extreme rain events over India in a warming environment. *Science* 314:1442–1445
- Goswami BN (1998) Interannual variations of Indian summer monsoon in a GCM: external conditions versus internal feedbacks. *J Clim* 11:501–522
- Goswami BN, Ajayamohan RS (2001) Intraseasonal oscillation and interannual variability of the Indian summer monsoon. *J Clim* 14:1180–1198
- Goswami BN, Shukla J (1984) Quasi-periodic oscillation in a symmetric general circulation model. *J Atmos Sci* 41:20–37
- Goswami BN, Xavier PK (2005) Dynamics of internal interannual variability of the Indian summer monsoon in a GCM. *J Geophys Res* 110:D24104. doi:10.1029/2005JD006042
- Grell GA (1993) Prognostic evaluation of assumptions used by cumulus parameterization. *Mon Weather Rev* 121:764–787
- Holtzlag AAM, Bruijn EIFD, Pan HL (1999) A high resolution air mass transformation model for short-range weather forecasting. *Mon Weather Rev* 118:1561–1575
- Kalnay E, Kanamitsu M, Kistler R, Collins W, Deaven D, Gandin L, Iredell M, Saha S, White G, Woollen J, Zhu Y, Leetmaa A, Reynolds R, Chelliah M, Ebisuzaki W, Higgins W, Janowiak J, Mo KC, Ropelewski C, Wang J, Jenne R, Joseph D (1996) The NCEP/NCAR 40-year reanalysis project. *Bull Am Meteorol Soc* 77:437–470
- Kang I-S, Ho C-H, Lim Y-K (1999) Principal modes of climatological seasonal and intraseasonal variations of the Asian summer monsoon. *Mon Weather Rev* 127:322–340
- Kiehl JT, Hack JJ, Bonan GB, Boville BA, Briegleb BP, Williamson DL, Rasch PJ (1996) Description of the NCAR community climate model (CCM3), Tech. rep., NCAR, NCAR/TN-420+STR
- Krishnan R, Kumar V, Sugi M, Yoshimura J (2009) Internal-feedbacks from monsoon-midlatitude interactions during droughts in the Indian summer monsoon. *J Atmos Sci* 66:553–578
- Kumar KK, Hoerling M, Rajagopalan B (2005) Advancing dynamical prediction of Indian monsoon rainfall. *Geophys Res Lett* 32:L08704. doi:10.1029/2004GL021979
- Lau KM, Yang GJ, Shen SH (1988) Seasonal and intraseasonal climatology of summer monsoon rainfall over east Asia. *Mon Weather Rev* 116:18–37
- Pal JS, Giorgi F, Bi X, Elguindi N, Solmon F, Gao X, Rauscher SA, Francisco R, Zakey A, Winter J, Ashfaq M, Syed FS, Bell JL, Diffenbaugh NS, Karmacharya J, Konar A, Martinez D, da Rocha RP, Sloan LC, Steiner AL (2007) Regional climate modeling for the developing world: the ICTP RegCM3 and RegCNET. *Bull Am Meteorol Soc* 88(9):1395–1409
- Rajeevan M, Bhate J, Kale JD, Lal B (2006) High resolution daily gridded rainfall data for Indian region: analysis of break and active monsoon spells. *Curr Sci* 9(3):296–306
- Ratnam JV, Giorgi F, Kaginalkar A, Cozzini S (2009) Simulation of the Indian monsoon using the RegCM3ROMS regional coupled model. *Clim Dyn* 33:119–139
- Ratnam JV, Kumar KK (2005) Sensitivity of the simulated monsoons of 1987 and 1988 to convective parameterization schemes in MM5. *J Clim* 18:2724–2743
- Reynolds RW, Rayner NA, Smith TM, Stokes DC, Wang W (2002) An improved in situ and satellite SST analysis for climate. *J Clim* 15:1609–1625

- Sperber KR, Palmer TN (1996) Interannual tropical rainfall variability in general circulation model simulations associated with the atmospheric model intercomparison project. *J Clim* 9:2727–2750
- Sugi M, Kawamura R (1997) A study of SST-forced variability and potential predictability of seasonal mean fields using the JMA global model. *J Meteorol Soc Jpn* 75:717–736
- Suhas E, Goswami BN (2008) Regime shift in Indian summer monsoon climatological intraseasonal oscillations. *Geophys Res Lett* 35:L20703. doi:[10.1029/2008GL035511](https://doi.org/10.1029/2008GL035511)
- Wang B, Ding Q, Joseph PV (2009) Objective definition of the Indian summer monsoon onset. *J Clim* 22:3303–3316
- Xavier PK, Marzin C, Goswami BN (2007) An objective definition of the Indian summer monsoon season and a new perspective on the ENSO–monsoon relationship. *Q J R Meteorol Soc* 133:749–764
- Wang B, Xu X (1997) Northern hemisphere summer monsoon singularities and climatological intraseasonal oscillation. *J Clim* 10:1071–1085